REPORT NO. 1836

THE ANALYSIS OF PILOT-PLANT PRODUCTS FOR COPPER, ZINC, AND LEAD WITH THE TELSEC LAB-X-250 ANALYSER

Director of Division T.W. Steele

Investigator G. Domel

Date 28th March, 1977

Project 08974

Project Report No. 1

NATIONAL INSTITUTE for METALLURGY

200 Hans Strydom Avenue
RANDBURG
2194 South Africa

NATIONAL INSTITUTE FOR METALLURGY

Report No. 1836

THE ANALYSIS OF PILOT-PLANT PRODUCTS FOR COPPER, ZINC, AND LEAD WITH THE TELSEC LAB-X-250 ANALYSER

28th March, 1977

Investigator: G. Domel

ISBN 0 86999 297 X

SYNOPSIS

Suites of sulphide material representative of copper, zinc, and lead concentrates, as well as 'intermediate' products, low-grade material, and tailing samples, were analysed with the Telsec Lab-X-250 Analyser, which is a radio-isotope X-ray-fluorescence instrument using 'balanced' filters for energy selection. A brief description of the instrument is given, stress being laid on the principle of 'balanced' filters. The determination of optimum instrumental parameters is described, and diagrams are provided to demonstrate the efficacy of energy selection.

Correlation diagrams are given for all three elements in each of the materials analysed. The scatter of data points encountered is examined in terms of possible spectral interference and matrix variation. It was found that, within specified limits of acceptability (5 per cent relative for concentrations above 10 per cent, and 0,5 per cent absolute for lower concentrations), all three elements could be determined satisfactorily in copper and lead concentrates and in low-grade material. Zinc concentrates could be analysed only for zinc.

The mechanisms of the spectral interference effects peculiar to the use of balanced filters are discussed, and a correction procedure is described and applied to improve the correlation for copper in the presence of a high zinc content. It is shown that the poor correlation found for 'intermediate' products and for lead in zinc concentrates is mainly due to matrix variations. The concentration range covered, the sensitivity, the precision, and, where applicable, the detection limits are tabulated for all three elements and all types of material analysed. A comparison of the results obtained with the Analyser and those obtained by atomic-absorption spectrophotometry is provided.

SAMEVATTING

Groepe sulfiedmateriaal wat verteenwoordigend is van koper-, sink- en loodkonsentrate, asook tussenprodukte, laegraadse materiaal en uitskotmonsters, is ontleed met die Telsec Lab-X-250-Analyser wat 'n radioisotoop-X-straalfluoressensie-instrument is wat van gebalanseerde filters gebruik maak vir energieseleksie. Daar word 'n kort beskrywing van die instrument gegee met spesiale klem op die beginsel van gebalanseerde filters. Die bepaling van die optimale instrumentele parameters word beskryf en diagramme word gegee om die doeltreffendheid van die energieseleksie te demonstreer.

Daar word korrelasiediagramme gegee vir al drie elemente in elkeen van die materiale wat ontleed is. Die verspreiding van datapunte wat teëgekom word, word ondersoek in terme van moontlike spektrale steuring en matriksvariasie. Daar is gevind dat al drie elemente, binne voorgeskrewe aanvaarbaarheidsgrense (5 persent relatief vir konsentrasies bo 10 persent, en 0,5 persent absoluut vir laer konsentrasies) bevredigend in koper- en loodkonsentrate en in laegraadse materiaal bepaal kan word. Sinkkonsentrate kan net vir sink ontleed word.

Die meganismes van die spektrale steuringseffekte eie aan die gebruik van gebalanseerde filters word bespreek en 'n korreksieprosedure word beskryf en toegepas om die korrelasie vir koper in die aanwesigheid van 'n hoë sinkinhoud te verbeter. Daar word getoon dat die swak korrelasie wat vir tussenprodukte en vir lood in sinkkonsentrate verkry word, hoofsaaklik aan matriksvariasies toe te skryf is. Die konsentrasiegebied wat gedek word, die gevoeligheid, die presisie en, waar dit van toepassing is, die opsporingsgrense word vir al drie elemente en al die soorte materiaal wat ontleed is, getabelleer. Daar word ook 'n vergelyking getref met die resultate wat met atoomabsorpsiespektrofotometrie verkry is.

CONTENTS

LIST OF ILLUSTRATIONS

1. INTRODUCTION

Previous work on a simple, portable radio-isotope-excited X-ray-fluorescence (RI-XRF) analyser[1] had shown that such instruments could be employed to advantage in circumstances where a close matching of calibration standards and samples is possible and where a certain degree of accuracy can be sacrificed in favour of the rapidity of on-the-spot analysis.

In 1974 a more sophisticated laboratory RI-XRF instrument, the Telsec Lab-X-250 Analyser, became available in the Republic of South Africa. Fitted with twin, sealed, gas-filled detectors, it offers improved energy resolution and line-to-background ratio. Its most striking feature, however, is a multiple-filter turret for rapid, easy, sequential determination of several different elements.

As the National Institute for Metallurgy (NIM) had need of on-the-spot analytical facilities for monitoring beneficiation work on sulphide materials, an application study was initiated to establish the capabilities of the Lab-X-250 with respect to the determination of copper, zinc, and lead in concentrates and allied flotation-test products. An accuracy of 5 per cent relative for concentration levels above 10 per cent absolute, and of 0,5 per cent absolute for lower concentration levels, was considered adequate for meaningful pilot-plant monitoring.

2. INSTRUMENTATION

Lab-X Analysers are a modular range of RI-XRF instruments that permit the determination of elements from silicon to uranium in liquids and solids[2].

2.1. Description of the Lab-X-250 Analyser

The Lab-X-250 Analyser used in the present work comprises a measuring head, a twin-channel electronics panel, and a programming unit, all housed in a bench-top cabinet. The measuring head consists of a sample-presentation turret, a radio-isotopic source mounted in a 'central-source' configuration (Figure 1), a turret containing up to six pairs of 'balanced' filters, and two sealed argon–methane detectors with their respective extra-high-tension (EHT) filters and preamplifiers. The properties of the 30 millibequerels (millicuries) of plutonium-238 source used are given in Table 1.

TABLE 1

Properties of the plutonium-238 radio-isotopic source

Radiation emitted	Uranium L X-rays
Energy of emitted radiation	12 to 21 keV
Half-life of isotope	86 years

The two 'balanced' filters constitute a filter pair, each filter being one half of a circular filter disc the diameter of which is slightly larger than that of the sample-holder. As shown in Figure 1, the filters are positioned so that the radiation impinging on detector A passes through the filter of higher atomic number ('total' count) and that falling on detector B passes through the filter of lower atomic number ('background' count). This system of adjacent placing of the two 'balanced' filters halves the counting time required for a difference count, but places higher requirements on the homogeneity and the even distribution of sample material in the sample-holder. Table 2 lists the filters used for the determination of iron, copper, zinc, and lead. (See Section 2.2 for a detailed discussion of 'balanced' filters.)

TABLE 2

Filters used for isolating the X-radiation of iron, copper, zinc, and lead

Element	Iron	Copper	Zinc	Lead
Characteristic radiation measured	Kα	Kα	Kα	Lα
Transmitting filter (A)	Mn	Ni	Cu	Ge
Absorbing filter (B)	Cr	Co	Ni	Ga

A single-channel pulse-height analyser (PHA) can be used in the 'threshold' mode to eliminate radiation of lower energy, or in the 'window' mode to reject radiation of energy lower and higher than the desired radiation. The window and the threshold are each controlled by a ten-turn potentiometer.

The pulses counted by the detectors, each of which has its own preamplifier, amplifier, and pulse-height analyser, are displayed on a ratemeter and are also passed to a scaler–timer with a digital display, which does not show the least significant digit. Counting times from 5 to 200 seconds can be selected. Different counting modes are available, allowing measurement of the pulses registered by counter A and counter B, measurement of the pulses registered by both counters (A+B), or direct measurement of the difference count (A–B). Long-term instrumental drift can be compensated for by a 'calibration' adjustment that can vary the counting time from +10 per cent to –10 per cent. The programming unit allows the above parameters to be preset for each filter pair and was used wherever possible for the sequential determination of several elements, which was quicker and less prone to human error.

Plastic sample-holders of 51 millimetres internal diameter, 33 millimetres in height, and fitted with a replaceable Mylar window, are supplied by the manufacturers.

2.2. Energy Selection by Means of 'Balanced' Filters

The energy spectrum of iron, copper, zinc, and lead obtained by the Lab-X-250 without the use of 'balanced' filters is shown in Figure 2, which demonstrates the serious overlap problems that exist in this spectral system. The resolution of the argon–methane detectors alone is such that the Kβ peaks for iron, copper, and zinc are not resolved from their respective Kα peaks but manifest themselves in the slight asymmetry of the Kα peaks. Escape peaks for the Kα radiations are visible.

'Balanced' filters are inexpensive means of discrimination against unwanted X-radiation and are therefore often incorporated in the less-expensive RI-XRF instruments. Their use is based on the fact that the mass-absorption coefficient at the K-absorption edge of a particular element increases suddenly by an order of magnitude as the energy increases through the absorption edge. Furthermore, any two adjacent elements have the following characteristics:

(1) K-absorption edges differing by only about 5 per cent in energy,
(2) K-absorption discontinuities of nearly equal magnitude, and
(3) closely similar variations of mass-absorption coefficients with energy in the region of the absorption edges[3].

Thus, the use of a pair of filters makes it possible for most of the energies above and below the required level to be absorbed (Figure 3).

By adjustment of the thickness of two filters having adjacent atomic numbers, the filters can be 'balanced' over a wide range of energies, except for the passband between the two absorption edges. The difference in transmittance between the two filters is then proportional to the X-ray intensity in the passband, i.e., the intensity of the desired element, which is transmitted by the filter of higher atomic number and absorbed by the filter of lower atomic number.

Figures 4 and 5 show the energy spectrum of a mixture of equal amounts of iron, copper, zinc, and lead oxides recorded with and without the use of 'balanced' filters, and demonstrate their effectiveness. However, the elimination of unwanted radiation is not complete, and, as the mechanism whereby matrix elements exert spectral interference in 'balanced' filter systems is peculiar to this technique of energy selection, it is considered in detail below. Spectral-energy data relevant to this discussion are given in Table 3.

The difference count (A–B), which is taken as a measure of the X-ray fluorescence intensity due to the desired element, is the arithmetical difference between the intensity of the radiation transmitted by the filter of higher atomic number (filter A) and that transmitted by the filter of lower atomic number (filter B), and is therefore dependent on the exact response of these filters to the impinging radiation. In the determination of zinc, for example, both Zn Kα and Zn Kβ radiation are excited in the sample. Filter A, made of copper, transmits Zn Kα radiation but absorbs Zn Kβ radiation and undergoes excitation, emitting Cu Kα and Cu Kβ radiation (see Table 3). The nickel filter (B), on the other hand, absorbs both Zn Kα and Zn Kβ radiation, emitting Ni Kα and Ni Kβ X-rays. The difference count (A–B) therefore comprises Zn Kα + Cu Kα + Cu Kβ – Ni Kα – Ni Kβ and is directly equivalent to the Zn Kα intensity emitted by the sample only insofar as the intensities of the characteristic X-rays emitted by the two filters are equal. Figure 6 is a graph of the intensity transmitted by the copper and nickel filters when zinc oxide is measured. The Zn Kα radiation transmitted by the copper filter, as well as the Ni K radiation emitted by the nickel filter, is clearly

TABLE 3

Spectral-energy data for some relevant metals

Element	K-absorption edge[4] keV	$K\alpha_{1,2}$ rays[5] keV	$K\beta_{1,3}$ rays[5] keV
Chromium	5,989	5,411	5,946
Manganese	6,540	5,894	6,489
Iron	7,112	6,398	7,057
Cobalt	7,709	6,924	7,648
Nickel	8,333	7,471	8,263
Copper	8,979	8,040	8,904
Zinc	9,659	8,630	9,570
Gallium	10,368	9,241	10,260
Germanium	11,104	9,874	10,980
	L_{III} absorption edge	$L\alpha_1$	$L\beta_{1,2}$
Lead	13,035	10,55	12,62

shown; the Cu K radiation emitted by the copper filter cannot be seen because it merges with the Zn Kα peak. The escape peak formed when the Zn Kα radiation excites Ar Kα rays in the detector gas is clearly visible.

Direct spectral interference is encountered when the characteristic X-radiation of a matrix element falls into the energy passband of the 'balanced' filters used. Thus, the presence of copper gives a positive bias in the determination of zinc because the Cu Kβ radiation is transmitted by filter A (copper) but not by filter B (nickel) (see Table 3). This effect is clearly demonstrated in Figure 7, where the intensity transmitted by the nickel filter does not show the asymmetry due to Cu Kβ radiation. It can also be seen that the copper filter transmits more Cu Kα than does the nickel filter, so that the positive difference count is due to both these effects.

Unequal transmission of unwanted radiation by the two 'balanced' filters occurs with any matrix elements having an atomic number lower than that of the filter elements. These differences in the degree of transmission can be corrected for by adjustment of the thickness of the filters. Thus, measurement of the Fe K radiation transmitted by the copper and the nickel filter would show a slightly higher intensity for the nickel filter because nickel has a lower mass-absorption coefficient for Fe K radiation than copper has. By use of the filter pair provided with the Lab-X-250, the opposite was found, presumably because the copper filter is thinner than the nickel filter (see Figure 8).

Where the energy of the unwanted radiation is sufficiently high, it is absorbed by the filter material and generates X-radiation characteristic of the filter material. Both the degree of absorption of the sample X-rays, as well as the intensity of the filter fluorescence, can be different for the two 'balanced' filters, thus giving rise to a further interference effect. For example, Pb Lα radiation is absorbed by both the copper and the nickel filter, but, as the Cu K-absorption edge is closer to the energy of the Pb Lα radiation than the Ni K-absorption edge is, a higher intensity of Cu K X-rays than of Ni K X-rays would be produced, so that there would be a positive effect on the difference count for zinc. However, some of the Pb L radiation is transmitted; Pb Lβ radiation, being of higher energy than Pb Lα, is transmitted to a greater extent than Pb Lα radiation. These effects are illustrated by Figure 9, which shows the response of the copper–nickel filter pair to Pb L radiation. Escape peaks from the interaction of both Cu K and Ni K radiation with the detector gas can be seen. Figure 9 also clearly demonstrates that the difference count is purely an arithmetical value and thus can be positive or negative, depending on the intensities transmitted by filters A and B.

The difference count for zinc for a sample containing zinc, copper, lead, and iron would therefore consist of the following:

Zn Kα from the sample
− Ni K generated by Zn Kα radiation
+ (Cu K–Ni K) generated by Zn Kβ radiation
+ (Cu Kα + Cu Kβ) transmitted by the copper filter
− Cu Kα transmitted by the nickel filter
− Ni K generated by Cu Kβ radiation
+ (Fe K radiation transmitted by the copper filter)
− (Fe K radiation transmitted by the nickel filter)
+ (Cu K–Ni K) generated by Pb L radiation
+ (Pb L radiation transmitted by the copper filter)
− (Pb L radiation transmitted by the nickel filter).

The intensity of the filter X-rays generated is related to the intensity of the radiation responsible for their excitation. Similarly, the intensity of interfering X-rays transmitted by a filter pair is proportional to the intensity of the impinging X-radiation. These two interfering effects can therefore be estimated and the difference count corrected accordingly.

Figure 10 summarizes the transmission characteristics of the copper–nickel filter pair with respect to iron, copper, zinc, and lead by showing plots of the difference counts only. However, when the spectral overlap reflected in Figure 10 is studied, it should be borne in mind that the situation is improved by the application of pulse-height analysis.

The determination of copper and lead is obviously subject to interference effects similar to those discussed for zinc. Figures 11 and 12 give the transmission characteristics of the nickel–cobalt filter pair and the germanium–gallium filter pair used for isolating Cu K and Pb L radiation respectively. As iron is present (up to 40 per cent) in the samples to be examined subsequently, the transmission characteristics of the manganese–chromium filter pair used for the determination of iron are given in Figure 13. As would be expected, spectral interferences are most marked when the concentration to be measured is low and that of the interfering element is very high in comparison and varies in magnitude.

3. EXPERIMENTAL METHOD

As the pure metals were not available, ferric oxide (Fe_2O_3), cupric oxide (CuO), zinc oxide (ZnO), and lead monoxide (PbO) were used in the setting up of the instrument and the determination of the optimum parameters for the measurement of Fe K, Cu K, Zn K, and Pb L X-radiation. Iron was included because of its considerable spectral significance in this work.

3.1. Synchronization of the Twin Detectors

The voltage of each detector was individually adjusted until maximum response was obtained for Cu K radiation at the centre of the energy range of the pulse-height analyser. The instrumental parameters used are given in Table 4. Figure 14 gives the resultant energy calibration of the PHA.

TABLE 4

Instrumental parameters for synchronization of the detectors

Material	CuO
Filters	None
Threshold	4,90
Window	0,20
Counting mode	A or B
Counting time	10 s

3.2. Optimization of the PHA Settings

With Figures 10 to 13 as a guide, a number of different threshold and window settings were chosen for each filter pair so that maximum sensitivity would be achieved for the element being determined with the minimum of interference from the associated elements.

All four oxides were measured with the filter pair for copper at the different settings by use of the (A−B) counting mode, and the sensitivity in counts per second for each per cent of copper was calculated. The copper equivalent of the different counts recorded for the other three oxides was calculated as follows:

$$\text{Copper equivalent} = \frac{\text{(A−B) for interfering element}}{\text{Counting time} \times \text{sensitivity for copper}}$$

The optimum setting chosen for copper was that which gave the highest ratio of copper sensitivity to the sum of the interferences expressed as copper equivalents. The procedure was repeated for lead, zinc, and iron. The optimum PHA settings arrived at are given in Table 5.

TABLE 5

Optimum PHA settings for iron, copper, zinc, and lead

Element	Fe	Cu	Zn	Pb
Threshold	2,8	4,0	5,0	6,2
Window	2,0	2,0	2,0	2,6

3.3. Presentation of the Sample Material

Powdered sample material was poured into the sample-holder provided with the instrument and distributed evenly over the entire surface of the Mylar window; this was done by tapping of the sample-holder vertically on to a flat surface. Repeated measurements after the sample-holder had been emptied and refilled did not indicate any differences that were statistically significant (see Section 3.4).

A sample depth of at least 10 mm is recommended by the manufacturers[6]. However, for the high-density metal concentrates under consideration, this frequently involved sample masses of up to 35 g. Under such a mass, the Mylar window of the sample-holder bulged progressively during measurement of the sample, thus leading to increasing intensity counts.

Experiments showed that 10 g of sample material produced an intensity count that did not increase significantly with an increase in sample depth. However, as it was difficult to ensure that this relatively small volume of material was spread uniformly over the whole area of the Mylar window, it was decided to standardize on a sample mass of 15 g.

Variations of X-ray intensity due to varying grain size was rendered negligible by the use of finely powdered material of closely similar grain size.

3.4. Precision of the XRF Measurements

A radio-isotope is considered a particularly stable source of exciting radiation, and consequently the precision of the fluorescence intensity is mainly a function of the counting statistics and the reproducibility of sample preparation and loading.

The emission of X-radiation, being a random phenomenon, follows the statistical laws of the Poisson distribution, the standard deviation (s) being defined as

$$s = \sqrt{N},$$

where N is the total number of counts accumulated. The precision associated with the difference count (A−B) is therefore given by the standard deviation of the intensity transmitted by filter A and that transmitted by filter B for the particular counting time used, i.e.,

$$s = \sqrt{(A+B)}.$$

For the purpose of the present work, in which the intensity measure used is the average of two

successive 50-second difference counts, the standard deviation of this mean, if counting statistics only are considered, is calculated as

$$s = \frac{\sqrt{(A+B) \text{ for } 100 \text{ seconds}}}{2}$$

$$= \frac{\sqrt{(A+B) \text{ for } 50 \text{ seconds}}}{\sqrt{2}}$$

So that an estimate could be made in a reasonably short time of the precision associated with a particular difference count, measurements in the (A+B) counting mode were made for 5 seconds and scaled up to the equivalent of a 50-second counting time.

3.5. Detection Limit

In X-ray-fluorescence analysis, the lower limit of detection is generally defined as that amount of element that gives a net intensity equal to twice the standard deviation of the background intensity. In RI-XRF analysis, where a direct difference count (A–B) is under consideration, zero concentration of the element is indicated when the intensity transmitted through filter A is the same as that transmitted through filter B. Hence,

$$\text{the lower limit of detection (\% element)} = \frac{2\sqrt{2B}}{T \times m},$$

where B is the intensity transmitted by filter B,
T is the counting time,
m is the sensitivity in difference counts per second for each per cent of the element.

3.6. Calibration of the Instrument

A series of flotation-test samples representative of the compositional range expected in the pilot-plant products were analysed for copper, zinc, and lead by an atomic-absorption method[7] accurate to within 3 per cent relative. The samples contained 0,01 to 30 per cent copper, 0,1 to 56 per cent zinc, and 0,1 to 85 per cent lead in varying proportions and in the presence of varying amounts of iron (up to 40 per cent). The main constituent minerals were pyrite, pyrrhotite, magnetite, chalcopyrite, galena, sphalerite, and quartz, which were present in varying proportions.

Duplicate measurements were taken of all the samples, the instrumental parameters summarized in Table 6 being used. Iron was included in the measurements because of its spectral significance in the XRF determination of copper, zinc, and lead.

TABLE 6

Optimized instrumental parameters

Element	Cu	Zn	Pb	Fe
Filter (A)	Ni	Cu	Ge	Mn
Filter (B)	Co	Ni	Ga	Cr
Threshold	4,0	5,0	6,2	2,8
Window	2,0	2,0	2,6	2,0
Counting modes	A–B and A+B			
Counting Times	50 s		5 s	

The duplicate difference counts were averaged and plotted against the concentrations determined by atomic-absorption spectrophotometry (AAS) (Figures 15 to 17). Best-fit lines calculated according to the least-squares method are given on the diagrams. The limits of acceptability, on either side of the best-fit line, are shown to indicate the degree of scatter acceptable at different concentrations.

In all instances, except in Figure 17, a linear relation between the difference count and the element concentration could reasonably be assumed and the coefficients of the equation

$$y = mx + c \quad \ldots\ldots (1)$$

were calculated according to the standard formulae[8]:

$$m = \frac{n.\Sigma(xy) - \Sigma x.\Sigma y}{n.\Sigma(y^2) - (\Sigma y)^2} \quad \ldots\ldots (2)$$

$$c = \frac{1}{n}(\Sigma x - m.\Sigma y), \quad \ldots\ldots (3)$$

where y is the difference count,
x is the concentration of the element,
m is the slope of the line, and
c is the intercept of the line on the y-axis.

Figure 17 presents a definitely curved graph due largely to the self-absorption of the lead. Here, the following equation was used[9]:

$$y = \frac{kx}{1 + \alpha x} \quad \ldots\ldots (4)$$

where y and x have the same meaning as above, and
k and α are empirically determined coefficients.

From equation (4),

$$\frac{x}{y} = \frac{1}{k} + \frac{\alpha}{k}.x. \quad \ldots\ldots (5)$$

By a least-squares fit of x/y versus x using equations (2) and (3) but with x/y substituted for y, c and m are evaluated and are used to give k and α:

$$k = 1/c \quad \ldots\ldots (6)$$
$$\alpha = km \quad \ldots\ldots (7)$$

All the calculations were done on an Olivetti Programma 602 desk-top computer.

3.6.1. *Grouping of Calibration Data*

It can be seen from Figures 15 to 17 that the scatter of the data points for all three elements exceeds the specified limits of acceptability (5 per cent relative at element concentrations above 10 per cent, and 0,5 per cent absolute for lower concentrations) in the lower concentration range, but that the data points in the upper concentration regions, corresponding to concentrates, are generally within specification. The scatter observed is due to a combination of spectral interferences (see Section 2.2), matrix absorption and enhancement effects exerted mainly by the four elements upon one another, and mineralogical effects due to the varying mineralogical composition of the sulphide material. In XRF analysis, errors due to these interference effects can largely be eliminated by the evaluation of sample intensities against intensities obtained from well-matched standards.

The sulphide-ore calibration standards used were therefore grouped according to the type of material, and new correlation diagrams were plotted for each element in each type of material (Figures 18 to 35). Table 7 outlines the criteria of classification and summarizes the concentration ranges of iron, copper, zinc, and lead encountered in each category. The actual limits between the different categories were decided upon empirically, and a reasonable amount of overlap must be expected.

TABLE 7

Classification of sample materials

Material	Criteria	Concentration ranges, %			
		Fe	Cu	Zn	Pb
Copper concentrate	Cu > 15 %	*ca* 15 to 30	15 to 29	2 to 13	1 to 15
Zinc concentrate	Zn > 30 %	*ca* 2	<0,1 to 2,5	33 to 56	< 1 to 20
Lead concentrate	Pb > 50 %	*ca* 2 to 15	< 0,1 to 5	1 to 9	53 to 83
Low-grade products	Cu, Zn, Pb < 10 %	*ca* 20	< 1 to 3	< 1 to 10	1 to 10
intermediate products	Cu up to 15 % Zn up to 30 % Pb up to 50 %	*ca* 15 to 30	0,1 to 15	3 to 30	1 to 45
Tailings	Spiked pilot-plant tailings	40	< 0.1 to 0.25	0.2 to 1.1	0.1 to 1.0

The correlation diagrams referring to the analysis of the different materials are discussed below, and the statistics for sensitivity, precision, and, where applicable, detection limit are summarized in Table 8.

3.6.1.1. Analysis of Copper Concentrates

It was found that, as the copper content increased during upgrading of the sulphide material, the zinc and lead contents generally decreased but the iron content increased (Figures 18 to 20). Almost all the samples studied followed this pattern, which accounts for the relatively good correlation between concentration and difference count shown by all three elements. All points fall within the acceptable limits, but, where the lead content is exceptionally high (25 per cent for the 20 per cent copper sample), the copper intensity is reduced owing to the increased mass absorption of the sample, and the data point falls close to the lower limit (see Figure 18).

3.6.1.2. Analysis of Zinc Concentrates

As the zinc increases, the iron decreases; the lead content, however, decreases both in magnitude and in extent of variation. Copper was very low throughout.

Zinc (Figure 21). All points fall within the acceptable limits. In the presence of high amounts of lead, the zinc intensity is suppressed owing to the increased mass absorption of the sample, e.g., the two data points closest to the lower limit represent samples having a lead content of up to 20 per cent.

Lead (Figure 22). The most striking feature of this diagram is the presence of negative difference counts. These are due to the difference in transmission of Zn K radiation by the gallium–germanium filters used for the determination of lead. The scatter, which is due to variations in the zinc contents with resultant variations in matrix and spectral interference effects, is pronounced.

Copper (Figure 23). The high difference count obtained for the very low concentrations of copper is evidence of severe spectral interference, mainly from zinc and iron, the two elements spectrally adjacent to copper and present in vastly larger concentrations than the copper. Variations in the concentration of these elements are responsible for the very bad scatter of the data points for copper. The determination of copper in zinc concentrates is therefore impossible at the low concentration levels required without correction for spectral interference.

3.6.1.3. Analysis of Lead Concentrates

As the lead concentration increases, the iron content decreases. Copper and zinc show no definite pattern but range from less than 1 to 5 per cent copper and from 1 to 8 per cent zinc. These variations account for the scatter of the points.

Lead (Figure 24). All the points are well within the limits, except for a sample having very low concentrations of copper and zinc and therefore having a higher lead intensity than the other samples owing to reduced mass absorption.

Zinc (Figure 25). One sample point falls just below the limit, being for a sample containing less copper

than most other samples. The correlation is considered adequate for analytical purpose.
Copper (Figure 26). All the points are within the limits. The high difference counts indicate strong positive spectral interference, mainly from lead but also from zinc.

3.6.1.4. Analysis of 'Intermediate' Products

These materials are intermediate between the concentrates and the low-grade products and can vary very widely in their concentrations of all four elements. They therefore at times exhibit both considerable spectral interference as well as marked, random matrix variations with concomitant pronounced scatter of the data points.
Copper (Figure 27). All the samples having high concentrations of zinc show the strong positive bias observed in zinc concentrates (Section 3.6.1.2), so that no confidence can be attached to results below about 2 per cent copper. For the rest of the samples, the correlation is acceptable.
Zinc (Figure 28). A large proportion of the points lie just outside the acceptable limits. This scatter is mainly due to variations in lead content, because samples of higher lead concentration show lower zinc intensity (see Section 3.6.1.2). High concentrations of copper, however, give an increased difference count. The effect of low mass absorption is particularly evidenced by the 29 per cent zinc sample which contains almost no lead and copper and hence has an exceptionally high zinc intensity.
Lead (Figure 29). Here the scatter due to matrix variations is very great. Usually, the higher the zinc concentration, the lower the lead intensity, but, as copper and iron have a similar effect on lead, only matrix correction can improve the correlation significantly.

3.6.1.5. Analysis of Low-Grade Products

In these samples the iron content is high (about 20 per cent) but relatively stable. The other three elements vary from less than 1 to 10 per cent for zinc and lead, and from less than 0,1 to 1 per cent for copper. The correlation is generally satisfactory.
Copper (Figure 30). Except for a sample in which zinc constitutes 10 per cent, remarkably good correlation was achieved, presumably owing to the buffering effect of the high but relatively constant iron content. At the low concentrations covered (less than 1,5 per cent copper), the acceptance limits would be meaningless and have therefore been omitted.
Zinc (Figure 31). Only one sample, with very low lead content, falls outside the limits, its lower mass absorption causing a higher zinc intensity.
Lead (Figure 32). All the points fall within the limits.

3.6.1.6. Analysis of Tailing Samples

The concentrations of copper, zinc, and lead in the tailing samples usually produced by the pilot plant were very low (copper 0,02 per cent, zinc 0,2 per cent, lead 0,15 per cent) and hardly varied. Previous measurements on such samples had all fallen within plus 2 or minus 2 standard deviations (based on counting statistics) so that, although it was obvious that these materials could not be analysed satisfactorily, no information on the sensitivity and detection limits could be obtained[10].

The suite of tailing samples examined in the present work was spiked with some sulphide material rich in copper, zinc, and lead so that the determination limit of the instrument could be determined. The iron content of these samples was very high (about 40 per cent) and varied so little that it not only provided a stable matrix but also maintained an acceptably constant positive spectral-interference effect on the three elements being determined. Figures 33 to 35 thus show a good correlation for increasing concentration of the elements being determined because, for each element, the concentration of all three interfering elements was kept largely constant. Sensitivity and detection limits, based on counting statistics, could be calculated.

The scatter at the lower end of each graph demonstrates the effect on the difference count of variation in the concentration of the interfering elements.

3.6.2. Statistical Assessment of the Correlation Diagrams

Table 8 summarizes the sensitivity, precision, and detection limits for Figures 18 and 35. The sensitivity is obtained direct from the slope of the best-fit line, which is expressed as difference counts per second for each per cent of the element.

The precision, based on counting statistics, was calculated from the (A + B) intensity measurements (see Section 3.4) and then expressed in terms of percentage element. This precision is the very best that can be obtained on the given sample material under the experimental conditions used, the

limiting factor being the intensity of the characteristic radiation and the presence of interfering elements. The same consideration applies to the detection limit, based on counting statistics (see Section 3.5), which assumes that the background measurement, consisting of the X-ray fluorescence due to matrix elements, will remain constant as the concentration of element to be determined increases.

For a more realistic forecast of the results to be expected under routine conditions when the best-fit lines are used as calibration graphs, the general scatter due to the different interference effects must be taken into account. The standard error of estimate[8] (S.E.) gives a measure of this scatter

$$\text{S.E.} = \sqrt{\frac{\Sigma(x-X)^2}{n-2}}, \quad \ldots\ldots (8)$$

where x is the concentration of the element as determined by AAS,
X is the concentration of the element as calculated from the best-fit line, and
n is the number of samples.

Similarly, the detection limit based on this scatter was calculated as 2 (S.E.) and therefore makes some allowance for fluctuations in the concentration of the interfering elements present.

TABLE 8

Determination of copper, zinc, and lead — statistical data

Material	Element	Concentration range of samples %	Sensitivity count/s/%	Standard deviation (based on counting statistics) % element	Standard error of estimate (S.E.) % element	Detection limit (based on S.E.) % element
Copper conct.	Cu	16 to 29	75	0,15	0,5	—
	Zn	2 to 13	83	0,11	0,2	—
	Pb	1 to 25	35	0,15	0,5	—
Zinc conct.	Cu	< 0,1 to 2,5	100	0,1	0,5	1
	Zn	33 to 56	100	0,12	0,9	—
	Pb	< 1 to 20	33	0,22	0,9	—
Lead conct.	Cu	< 0,1 to 5	80	0,1	0,3	0,6
	Zn	1 to 9	85	0,1	0,3	0,6
	Pb	53 to 83	25	0,4	0,8	—
Intermediate products	Cu	0,1 to 15	80	0,12	0,5	1
	Zn	3 to 30	80	0,10	0,7	—
	Pb	1 to 45	35	0,22	3,3	—
Low-grade products	Cu	< 1 to 3	130	0,08	0,1	0,2
	Zn	< 1 to 10	120	0,05	0,3	0,6
	Pb	1 to 10	50	0,10	0,3	0,6
Tailings	Cu	< 0,1 to 0,25	150	0,05	0,1	0,2
	Zn	0,2 to 1,1	110	0,025	0,05	0,1
	Pb	0,1 to 1,0	75	0,02	0,03	0,06

4. APPLICATION OF THE LAB-X-250 ANALYSER AT NIM

To date, the instrument has been used satisfactorily for the routine analysis of the following pilot-plant products:

copper concentrates for copper, zinc, and lead
zinc concentrates for zinc
lead concentrates for copper, zinc, and lead
plant feeds for zinc and lead.

Approximately 15 g of sample material are measured, the instrumental parameters given in

Table 6 being used. The difference counts are evaluated, the best-fit lines given in the relevant diagrams being used as calibration curves. The synchronization of the detectors is checked daily, and the 'calibration' control is used to ensure that the slope of the calibration graphs has not shifted.

Table 9 lists the reproducibility obtained when several samples were analysed daily over a one-month period. Table 10 gives a recent comparison of results obtained by AAS and by RI-XRF. The copper content of the particular run of lead concentrates was below the RI-XRF detection limit.

TABLE 9

Reproducibility of RI-XRF results

Element	Concentration level %	Theoretical standard deviation (based on counting statistics) % absolute	Actual standard deviation (n=15) % absolute
Copper	25	0,15	0,5
Zinc	50	0,12	0,6
	4	0,11	0,3
Lead	75	0,4	0,9
	7	0,1	0,2

TABLE 10

Comparison of AAS and RI-XRF results
(based on the analysis of 11 batches of material)

Material	Element	Concentration range	Average deviation	Standard deviation of the difference
		% element		
Copper concl.	Cu	16 to 26	0,7	1,1
	Zn	6 to 12	0,4	0,6
	Pb	2 to 7	0,1	0,9
Zinc concl.	Zn	41 to 53	−0,5	1,4
Lead concl.	Zn	2 to 4	0,2	0,3
	Pb	64 to 73	1,5	1,7
Feeds	Zn	1,5 to 2,1	−0,15	0,14
	Pb	3,1 to 3,9	−0,1	0,1

As can be seen from the results presented in Tables 9 and 10, both the reproducibility and the accuracy are within the required limits.

The application of the Lab-X-250 Analyser to the analysis of bench-test samples has been less successful because that type of investigational work requires greater accuracy and also involves products that can vary widely and randomly in their relative proportions of iron, copper, zinc, and lead.

5. DISCUSSION

Good correlations were obtained between the difference counts and the concentrations of the major elements in the three concentrates, i.e., copper, lead, and zinc, because at these high concentrations spectral interference and matrix effects from the minor constituents are negligible. However, the correlation for the intermediate products is poor because of the effects of random variations in matrix composition, and hence also of spectral interference. Whereas at high

concentrations the precision of the RI-XRF measurements is about 0,5 per cent relative, the relative precision at low concentrations is poor because a small difference count (A–B) is associated with a high total (A + B) count (see Section 3.4). Either positive or negative interferences, which may be of a large magnitude, can occur. This is indicated by the varying intercepts obtained on the y-axis of the best-fit lines, and, only where the concentration of the interfering element (or elements) remains relatively constant, is good correlation achieved, e.g., in the analysis of low-grade materials. For a good correlation on a wider basis, and therefore improved analytical results, elimination of, or correction for, interference and matrix effects is necessary.

Another possible source of error is the presence of mineralogical effects — the phenomenon in which the same concentration of element produces different fluorescence intensities depending on the mineral in which it is present. Errors arising from this phenomenon would be expected for iron but are considered negligible for copper, lead, and zinc, almost all of which occur in single mineral forms, e.g., chalcopyrite, sphalerite, and galena respectively.

Spectral interference can be corrected by means of the following simultaneous equations, which give the relation between the measured (M) and the 'true' (T) difference count for each element.

$$Fe_T = Fe_M - [(Cu_T F_{Fe,Cu}) + (Zn_T F_{Fe,Zn}) + (Pb_T F_{Fe,Pb})] \quad \ldots\ldots (9)$$

$$Cu_T = Cu_M - [(Fe_T F_{Cu,Fe}) + (Zn_T F_{Cu,Zn}) + (Pb_T F_{Cu,Pb})] \quad \ldots\ldots (10)$$

$$Zn_T = Zn_M - [(Fe_T F_{Zn,Fe}) + (Cu_T F_{Zn,Cu}) + (Pb_T F_{Zn,Pb})] \quad \ldots\ldots (11)$$

$$Pb_T = Pb_M - [(Fe_T F_{Pb,Fe}) + (Cu_T F_{Pb,Cu}) + (Zn_T F_{Pb,Zn})] \quad \ldots\ldots (12)$$

$F_{Fe,Cu}$, etc. are correction factors embodying the total spectral interference effect exerted by the interfering element (e.g., Cu) on the element being determined (e.g., Fe), irrespective of which mechanism is involved (see Section 2.2).

These interference factors are readily determined experimentally by measurement of all four oxides through each of the four filter pairs at the same instrumental settings as were used for the measurement of the samples. The factors are then calculated as follows.

Example

$$F_{Fe,Cu} = \frac{\text{(A − B) for copper oxide through the filter pair for iron}}{\text{(A − B) for copper oxide through the filter pair for copper}}$$

The factors determined in this study for the particular instrument, filter pairs, and measurement parameters used range from –0,02 for the effect of zinc on lead to +0,16 for the effect of lead on zinc.

Corrections for spectral interference were applied to the intensity data presented in Figures 18 to 35 by solving of equations (9) to (12) by iteration with the use of an Olivetti Programma 602 desk-top computer. As expected, all the best-fit lines were shifted closer to the origin, and negative difference counts were eliminated. However, significant improvement in the scatter of the data points was obtained only where the concentration of the element being determined was very low and that of the interfering element (or elements) very high in comparison, e.g., copper in zinc concentrates (see Figure 36) and the very low copper in 'intermediate' products (see Figure 37).

The scatter remaining after correction for spectral interference must be largely attributed to the presence of randomly varying mutual absorption and enhancement effects exerted by the elements upon one another. This assumption can be confirmed for the absorption effects by correction of the difference counts first for spectral interference and then, by means of published mass-absorption coefficients[11], for variations in the mass absorption of the sample matrix. For the latter, the standard formula

$$C_i = D.I_i.\Sigma(\mu_i W_i) \quad \ldots\ldots (13)$$

was used, where

C_i is the concentration of the element being determined,
D is a proportionality constant,
I_i is the fluorescent intensity of the element being determined, and
$\mu_i W_i$ is the product of the mass-absorption coefficient of element i for the characteristic radiation of the element being determined (μ_i) and the mass fraction of the element i present(W_i); $\mu_i W_i$ must be calculated for each element present in the sample.

As the total composition of the samples was not known, the mutual-absorption effects of only iron, copper, zinc, and lead were considered. The exact iron content of the samples was also not known and had to be roughly determined by comparison of their difference counts with those of sulphide-ore products of known iron content. Despite these limitations, a graph (Figure 38) of the matrix-corrected intensities, $I_i.\Sigma(\mu_i W_i)$, plotted against the lead concentration shows a linear correlation with a standard error of estimate of 1.2. This represents a statistically significant improvement on the correlation shown by the uncorrected intensities (Figure 17), the standard error of estimate of which is 2.6.

This proves that the correction of the difference counts for spectral interference and matrix effects would lead to significant improvement in the accuracy of analytical results. It is also expected that the greater tolerance to variations in matrix composition would permit the extension of the compositional range of the standards and samples, so that intermediate products and bench-test samples could be analysed satisfactorily. Work on the application of matrix correction by the use of influence factors, which would compensate for absorption as well as enhancement effects, is at present being undertaken. However, it must be borne in mind that the use of such corrections needs computer facilities, thus negating the basic simplicity of the original concept.

6. CONCLUSIONS

A Lab-X-250 Analyser is suitable for on-the-spot pilot-plant monitoring of the following materials within the specified limits of acceptability (5 per cent relative for element concentrations above 10 per cent, and 0.5 per cent absolute for lower concentrations) provided that well-matched calibration standards are used and the concentration of the element to be determined is above about 1 per cent:

copper concentrates for copper, zinc, and lead
lead concentrates for copper, zinc, and lead
zinc concentrates for zinc
low-grade material for copper, zinc, and lead.

For the satisfactory determination of copper and lead in zinc concentrates, and of copper, lead, and zinc in intermediate products and bench-test samples, corrections must be applied for spectral interference and matrix variations. Where the concentration of the element to be determined is very low, the scatter due to the counting statistics alone is bad and it is doubtful whether meaningful results can be obtained for tailing samples even after corrections have been made for interferences.

7. REFERENCES

1. DOMEL, G., and STEELE, T.W. The use of the Ekco Mineral Analyser for the determination of copper and zinc in the presence of iron. Johannesburg, National Institute for Metallurgy, *Report no. 1430*. 27th Jun., 1972.
2. TELSEC INSTRUMENTS LTD. The Lab-X range of radio-isotope excited X-ray fluorescence analysers. Oxford.
3. CAMERON, J.F., and RHODES, J.R. Filters for energy selection in radioisotope X-ray techniques. *ENCYCLOPEDIA OF X-RAYS AND γ-RAYS*. New York, Reinhold, 1963. pp. 387–392.
4. WOLDSETH, R. All you ever wanted to know about X-ray energy spectrometry. California, Kevex Corp., 1973.
5. WHITE, E.W., and JOHNSON, G.G. X-ray emission and absorption wavelengths and two-theta tables. *ASTM Data Series DS37A*. Philadelphia, American Society for Testing and Materials, 1970.

6. TELSEC INSTRUMENTS LTD. The Lab-X range of radioisotope excited X-ray fluorescence analysers — Lab-X instruction manual. Oxford.
7. WALL, G., and STEELE, T.W. The determination, by atomic-absorption spectrophotometry, of copper, lead, and zinc in sulphide concentrates. Johannesburg, National Institute for Metallurgy, *Report no. 1798*. 29th Jan., 1976.
8. DOWNIE, N.M., and HEATH, R.W Basic statistical methods. New York, Harper & Row Publishers, 1970. pp. 129–139.
9. DOMEL, G., RUSSELL, B.G., and STEELE, T.W. The determination by X-ray fluorescence spectrometry of minor amounts of niobium and tantalum in geological materials. Johannesburg, National Institute for Metallurgy, *Report no. 1514*. 18th Apr., 1973.
10. DOMEL, G. The analysis of flotation-test samples by means of the Telsec Lab-X-200 analyser (a preliminary application study). Johannesburg, National Institute for Metallurgy, *Technical Memorandum, Analytical no. 70*. 21st Aug., 1974. (Not published.)
11. BIRKS, L.S. Electron probe microanalysis. New York, Interscience Publishers, 1963.

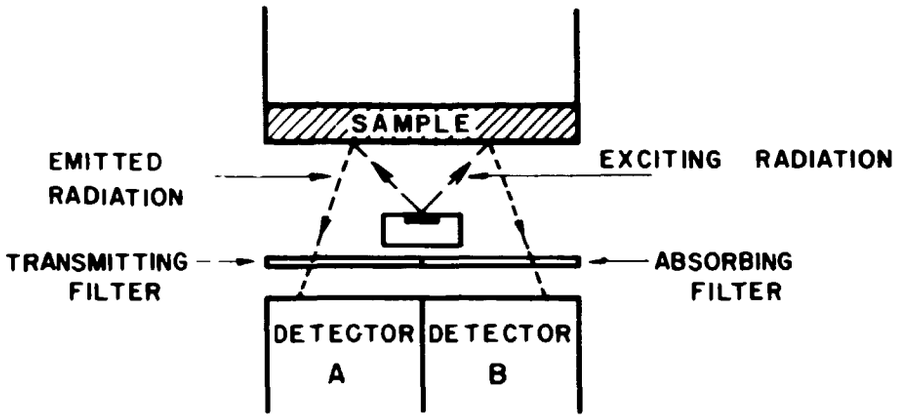

FIGURE 1 The 'central source' configuration of the Telsec Lab-X-250 Analyser.

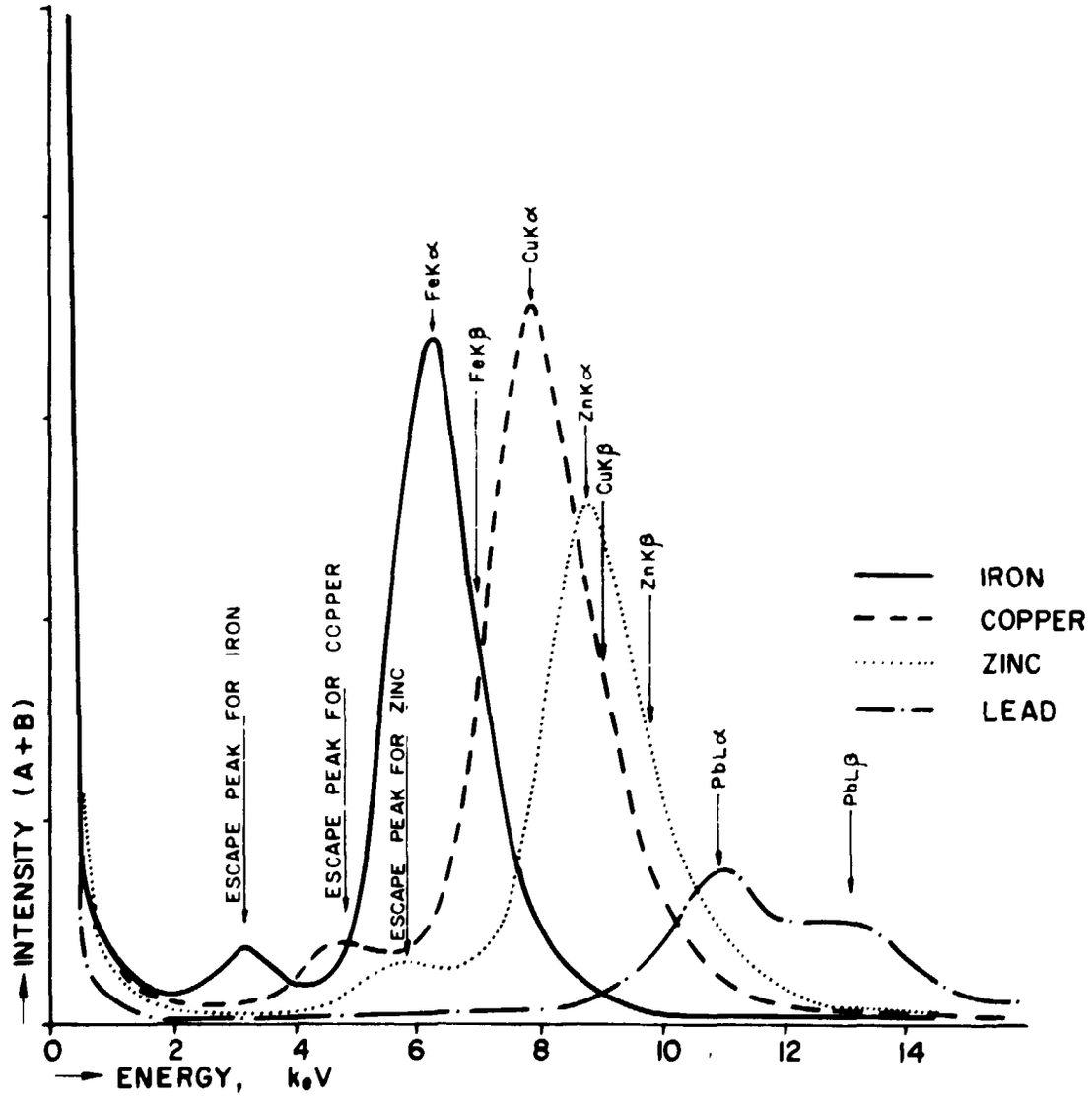

FIGURE 2 Energy spectra for iron, copper, zinc, and lead

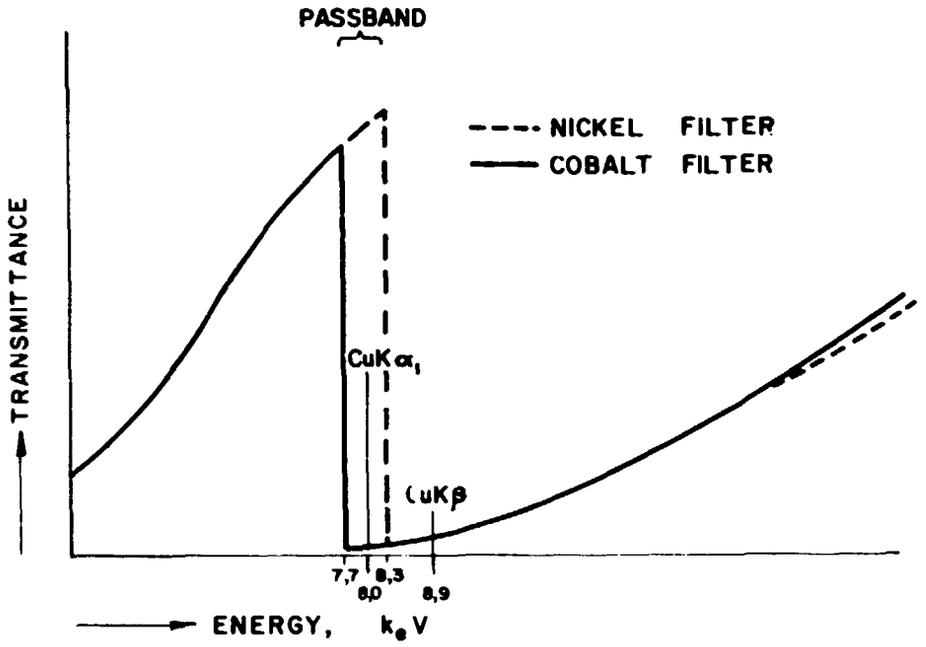

FIGURE 3 The use of 'balanced' filters for the isolation of Cu K_α energy

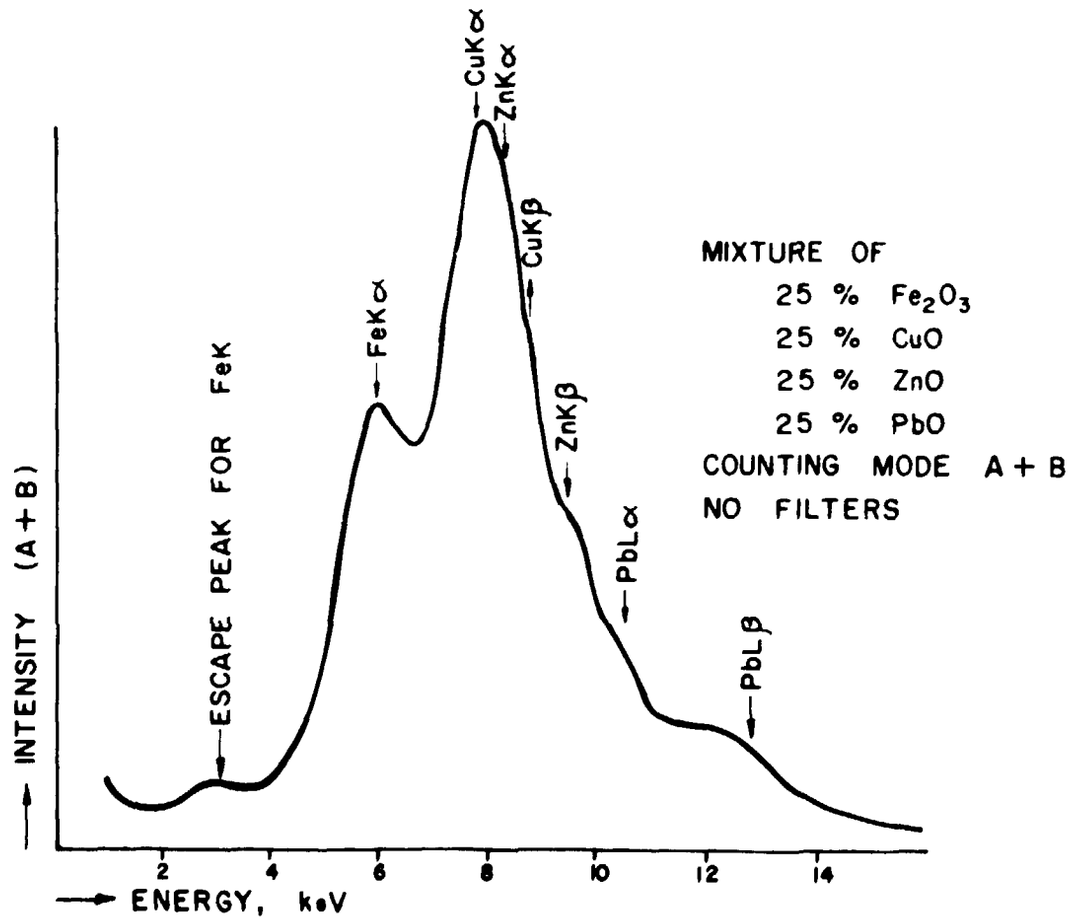

FIGURE 4 Unresolved energy spectrum for oxide mixture

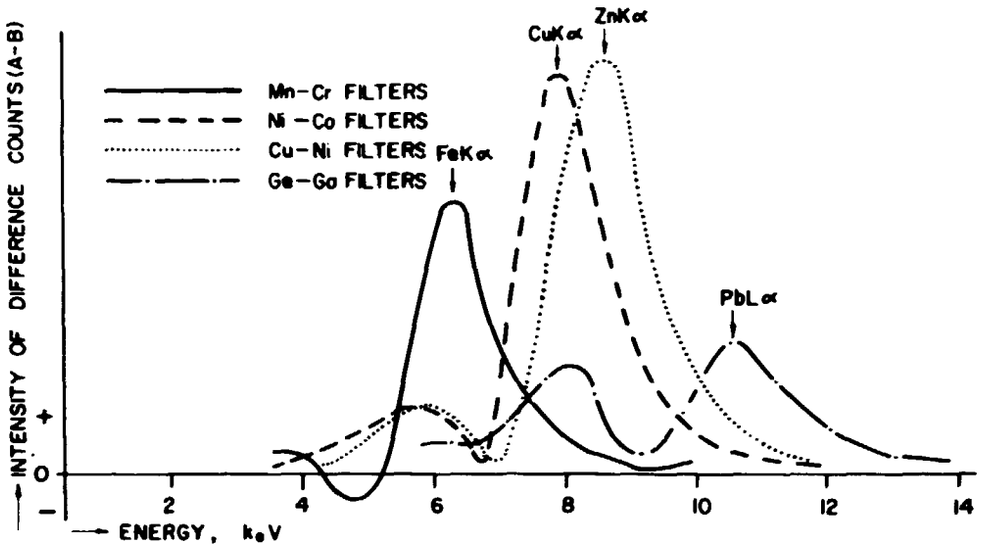

FIGURE 5 Energy spectrum for oxide mixture resolved by means of 'balanced' filters

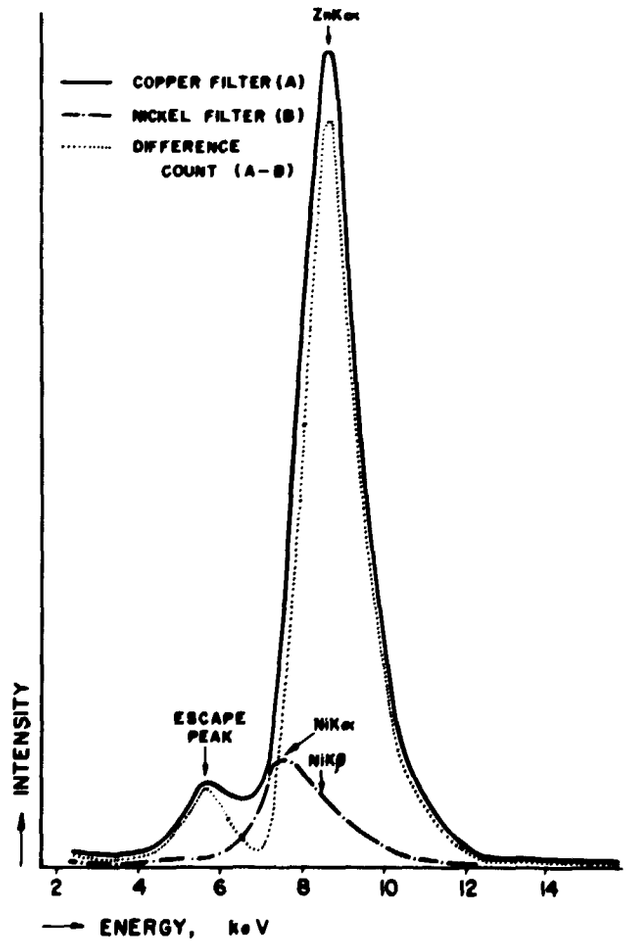

FIGURE 6 Response of copper-nickel filter pair to Zn K radiation

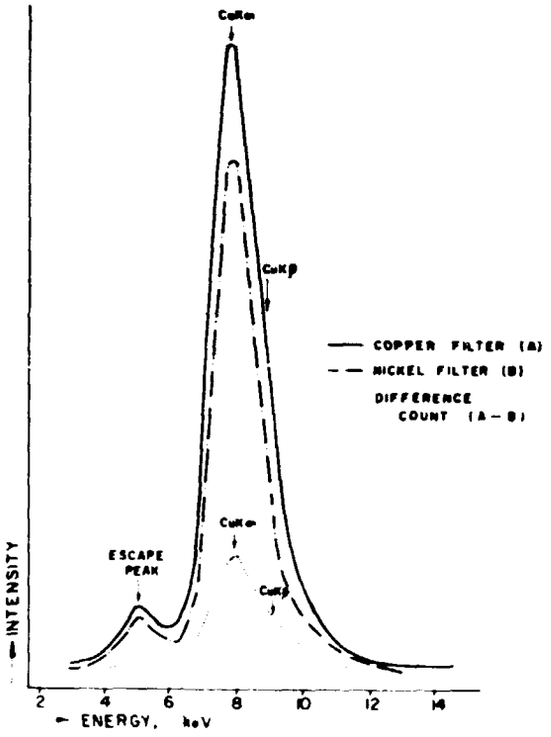

FIGURE 7 Response of copper–nickel filter pair to Cu K radiation

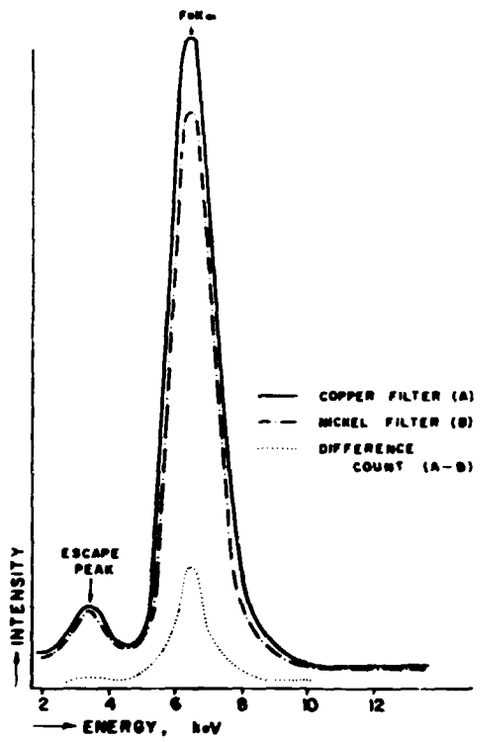

FIGURE 8 Response of copper–nickel filter pair to Fe K radiation

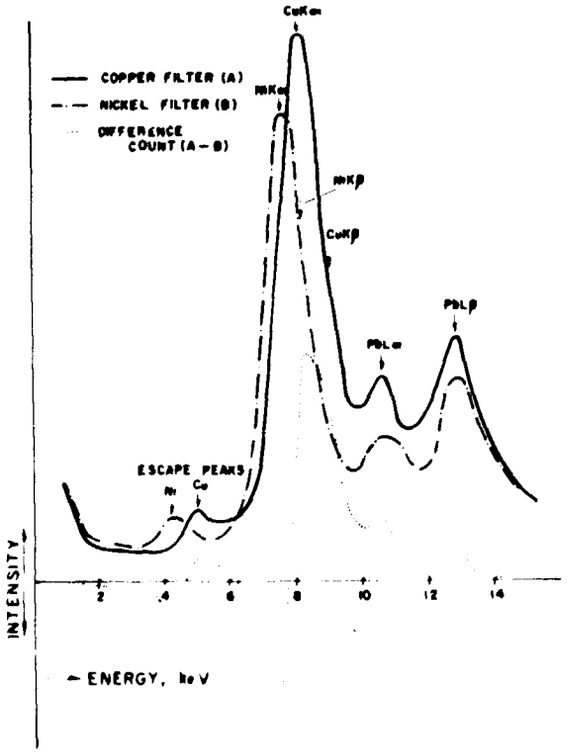

FIGURE 9 Response of copper–nickel filter pair to Pb L radiation

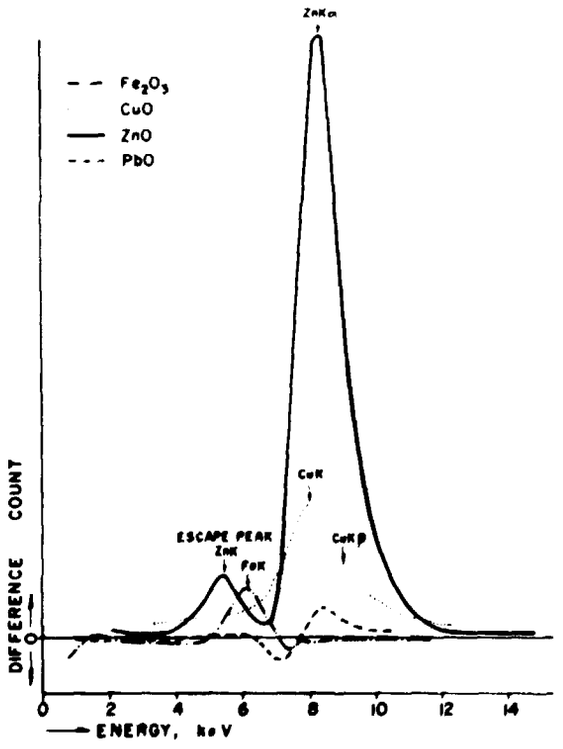

FIGURE 10 Transmission characteristics of the copper–nickel filter pair

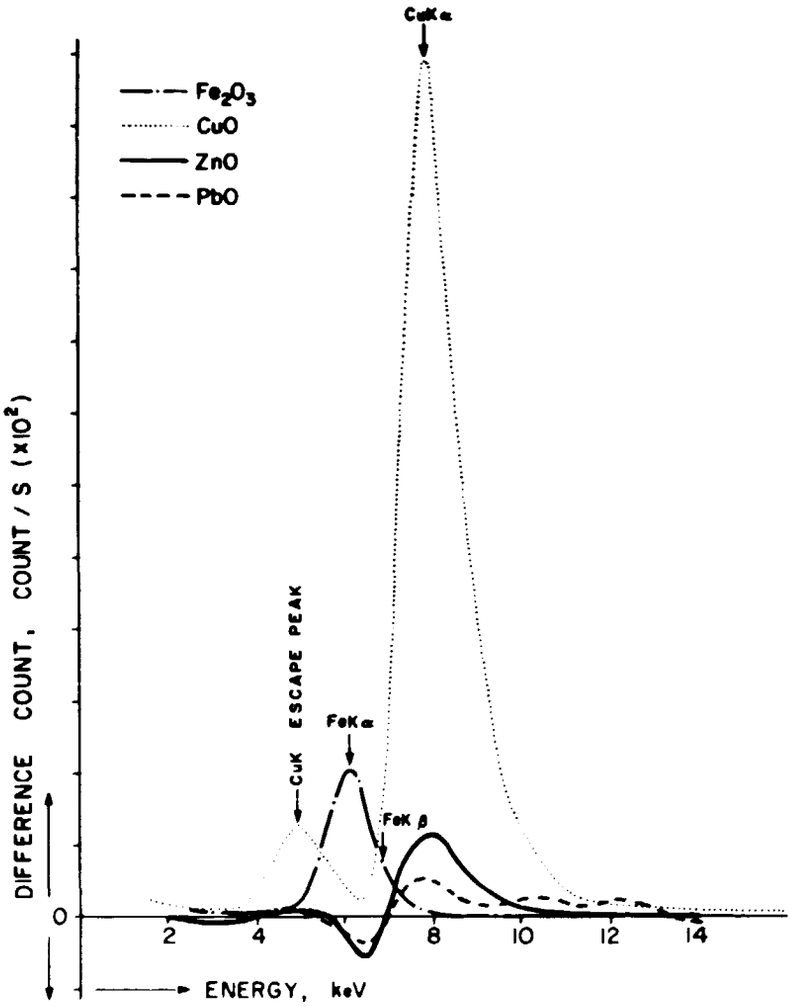

FIGURE 11 Transmission characteristics of the nickel–cobalt filter pair

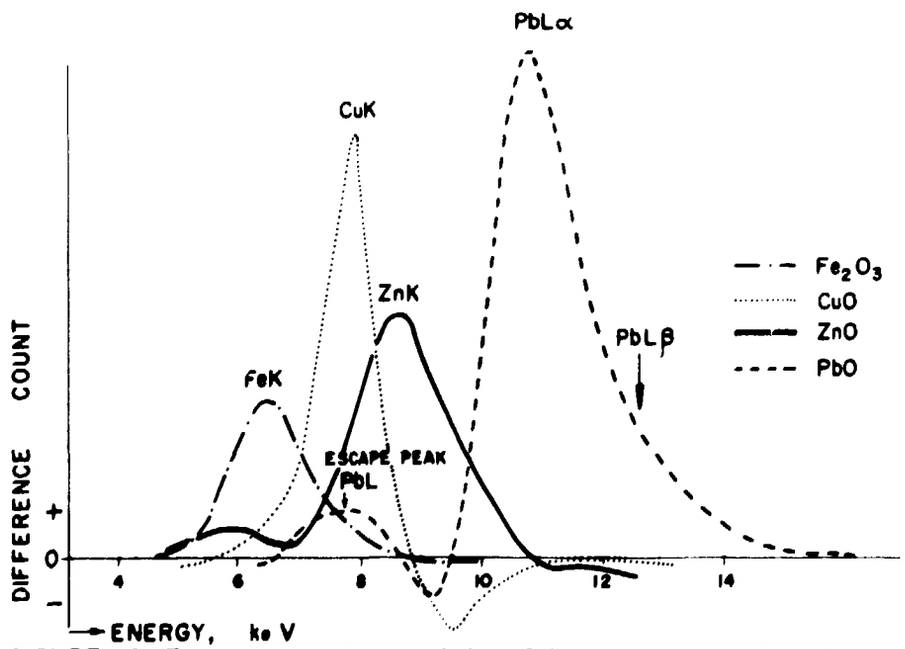

FIGURE 12 Transmission characteristics of the germanium–gallium filter pair

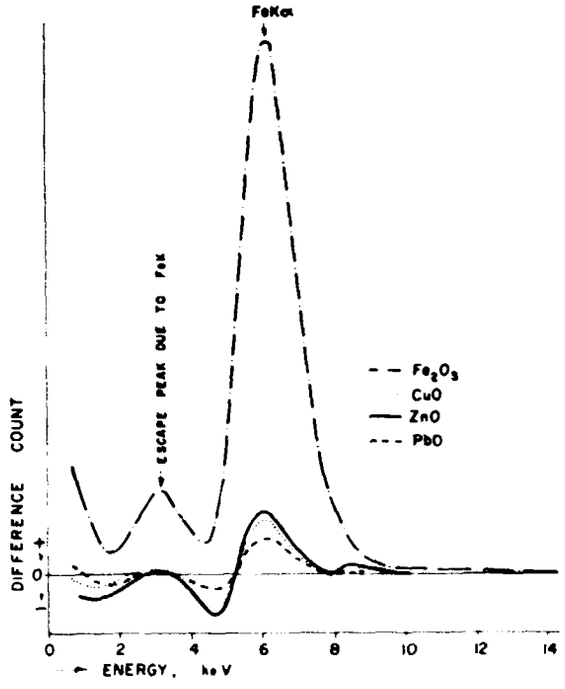

FIGURE 13 Transmission characteristics of the manganese–chromium filter pair

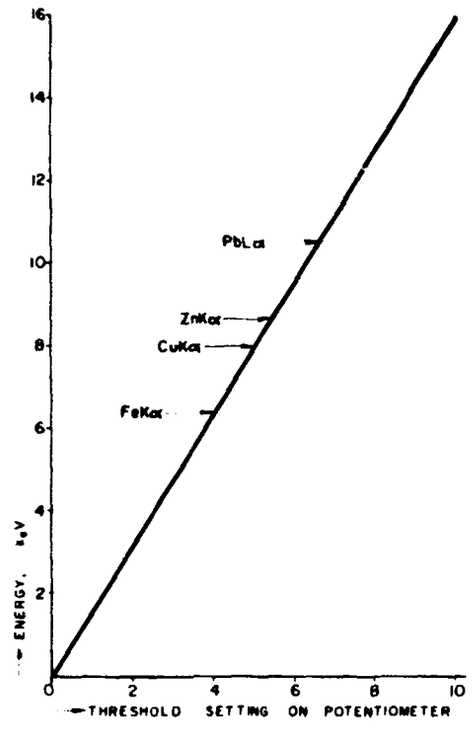

FIGURE 14 Calibration of pulse–height analyser

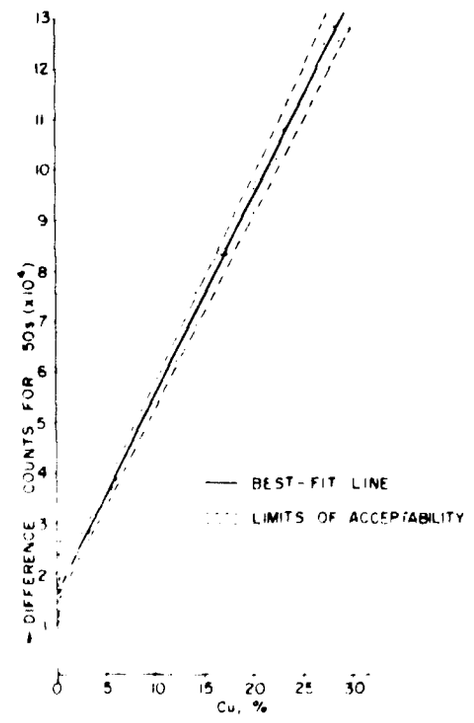

FIGURE 15 The analysis of sulphide ore products for copper

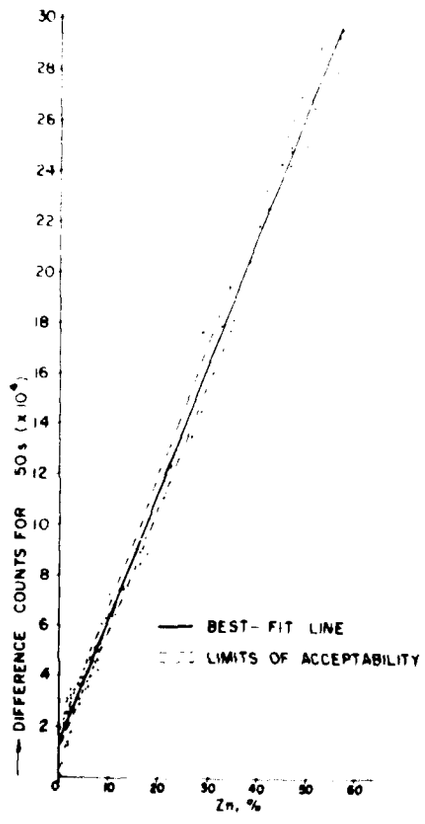

FIGURE 16 The analysis of sulphide ore products for zinc

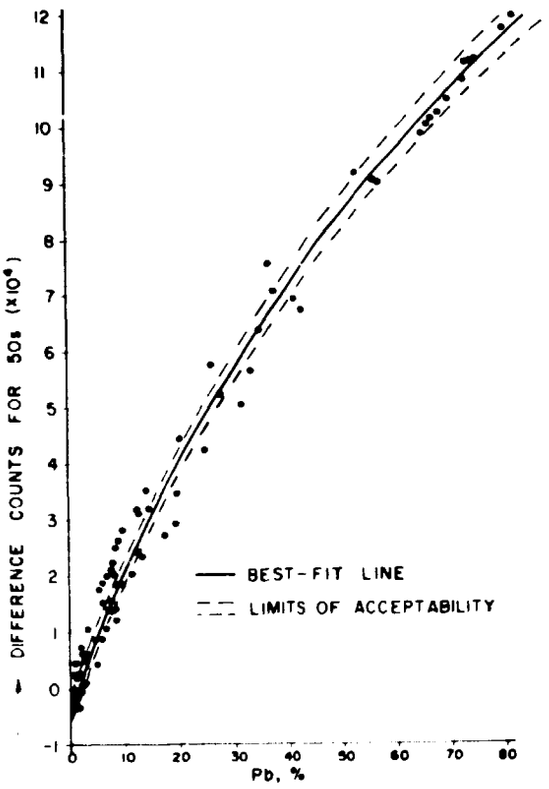

FIGURE 17 The analysis of sulphide ore products for lead

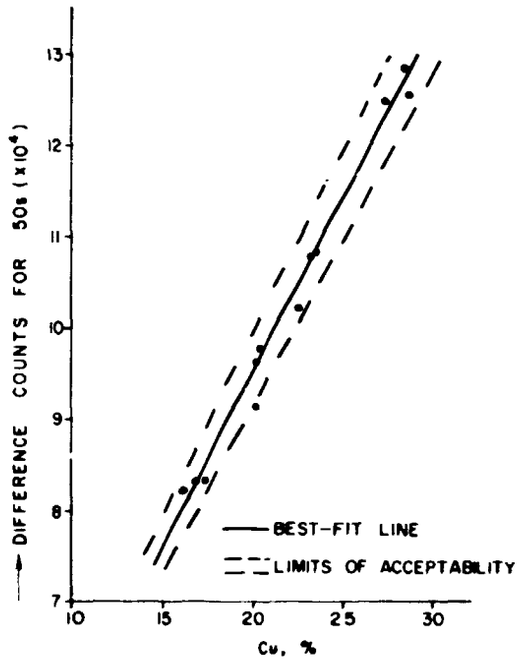

FIGURE 18 The determination of copper in copper concentrates

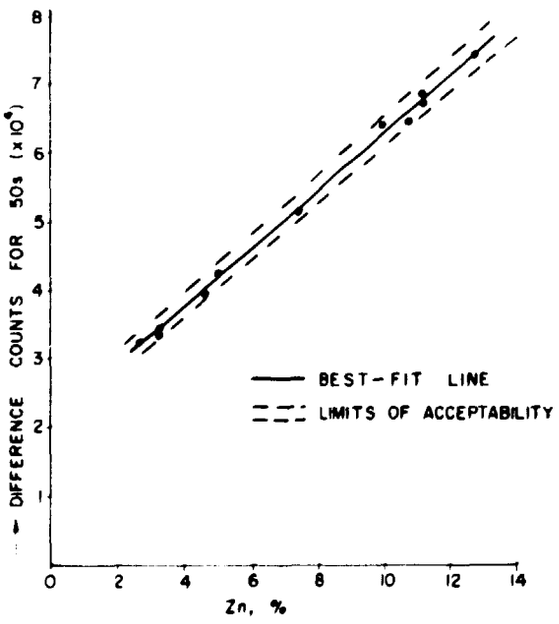

FIGURE 19 The determination of zinc in copper concentrates

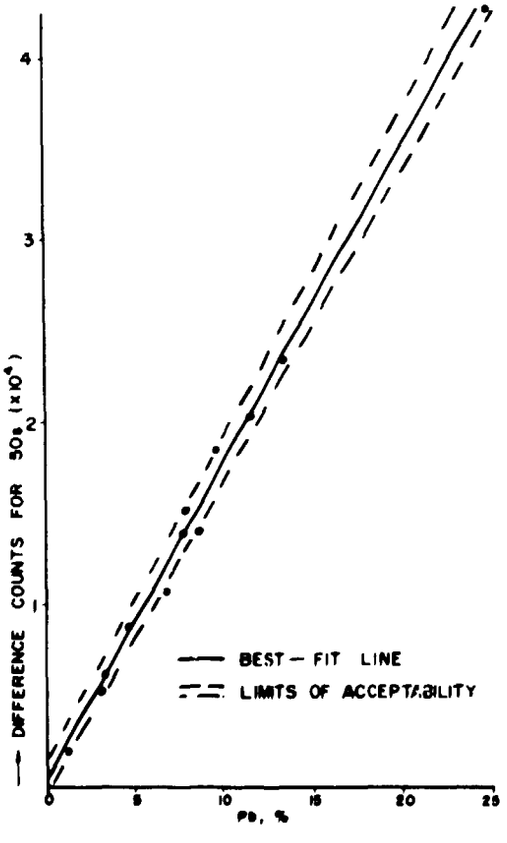

FIGURE 20 The determination of lead in copper concentrates

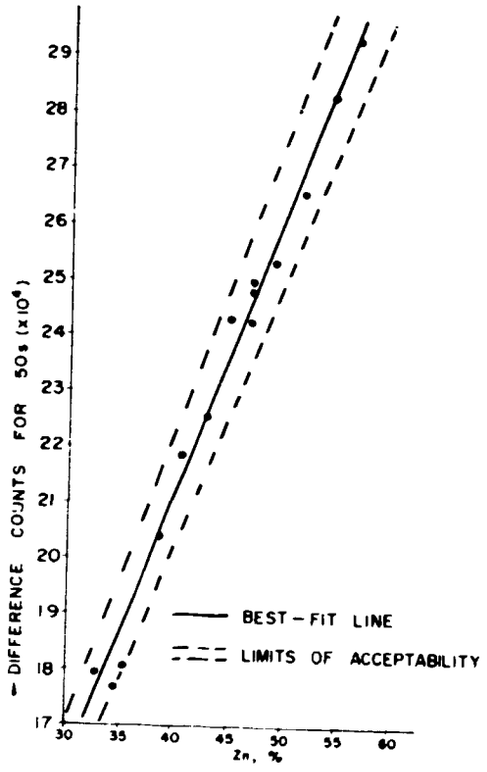

FIGURE 21 The determination of zinc in zinc concentrates

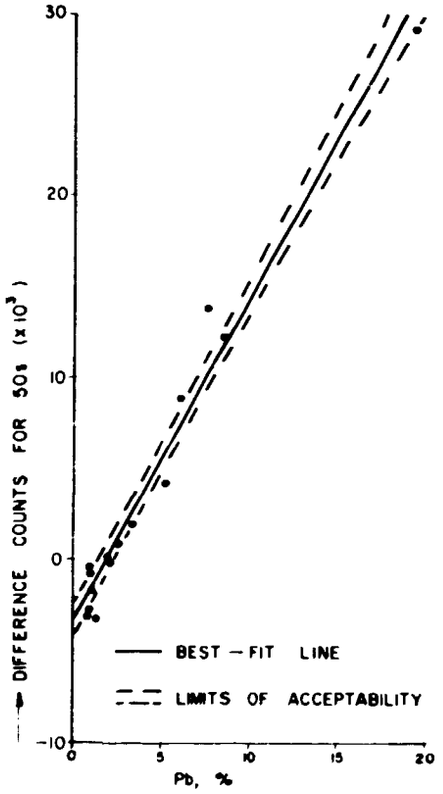

FIGURE 22 The determination of lead in zinc concentrates

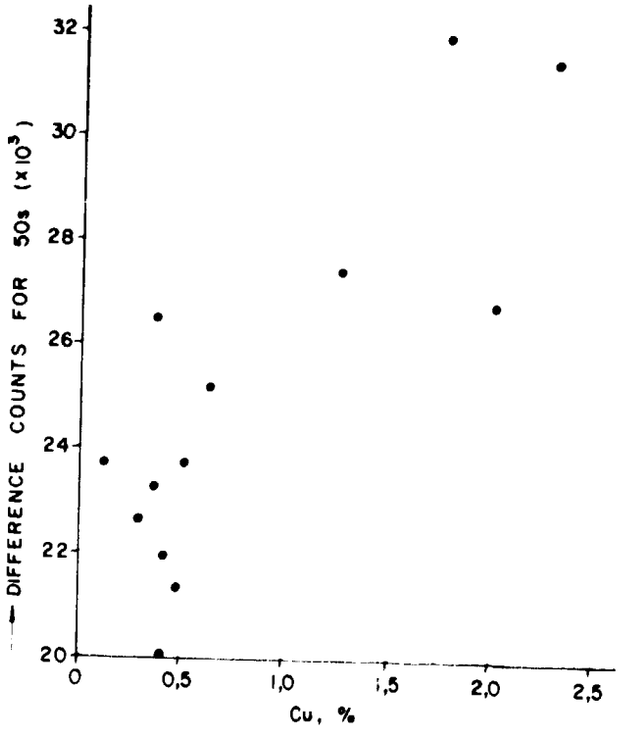

FIGURE 23 The determination of copper in zinc concentrates

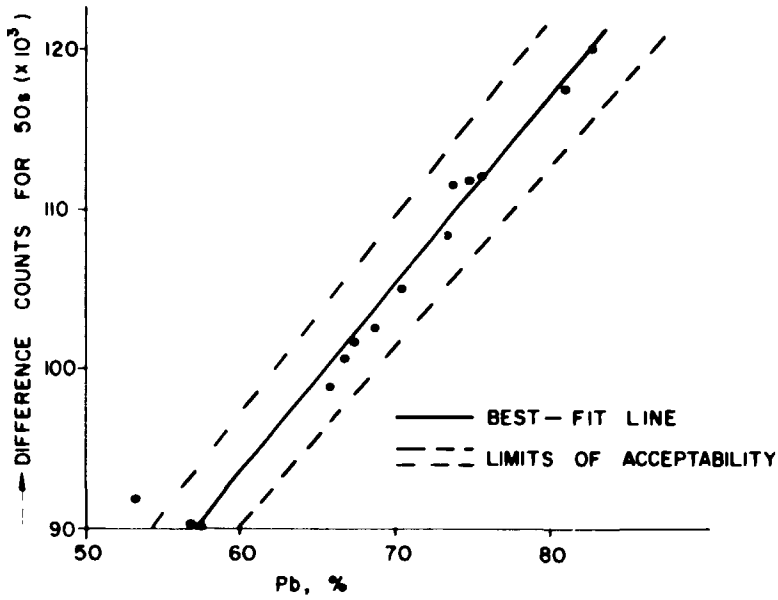

FIGURE 24 The determination of lead in lead concentrates

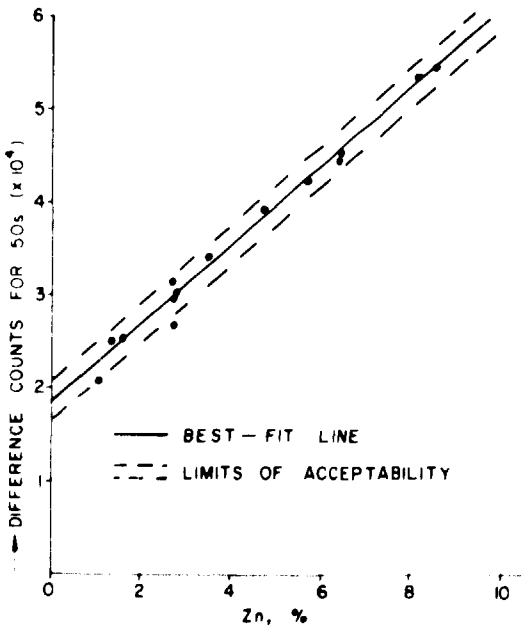

FIGURE 25 The determination of zinc in lead concentrates

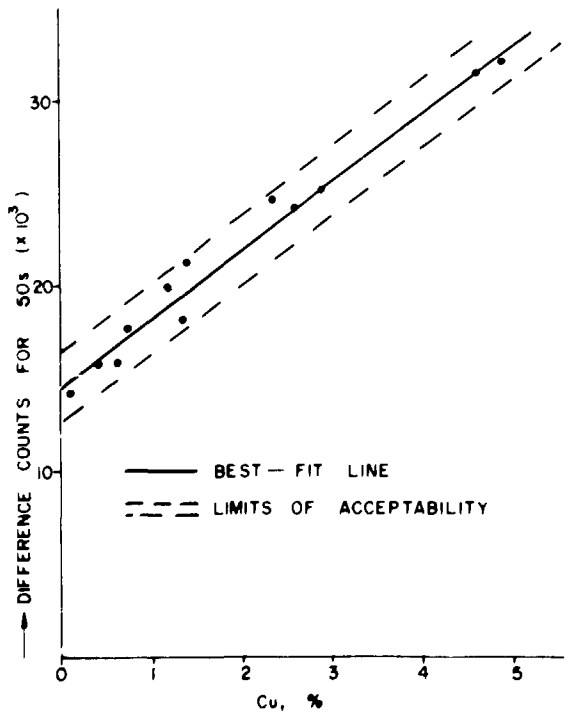

FIGURE 26 The determination of copper in lead concentrates

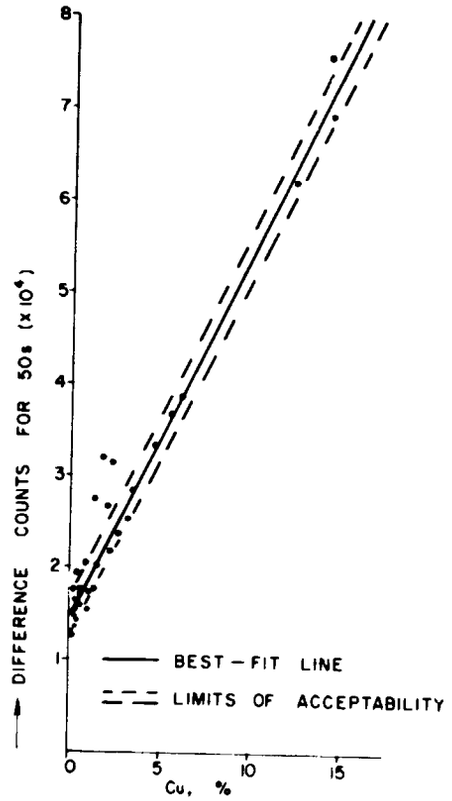

FIGURE 27 The determination of copper in 'intermediate' products

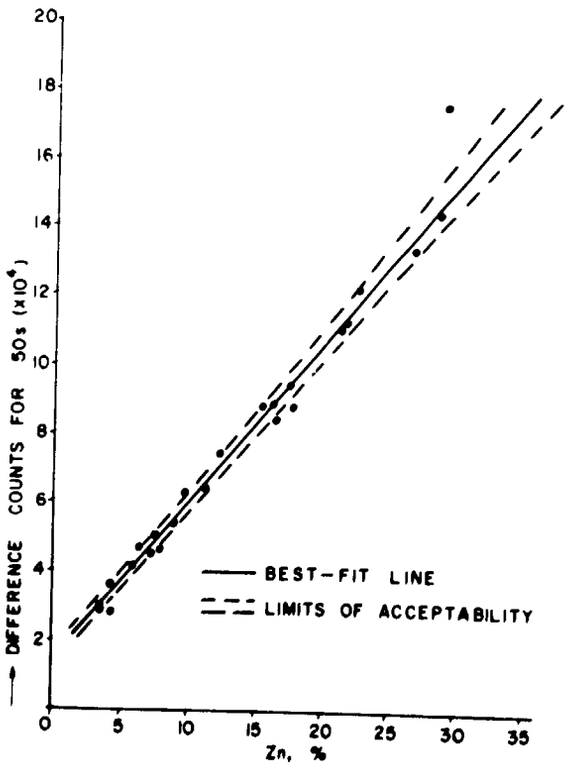

FIGURE 28 The determination of zinc in 'intermediate' products

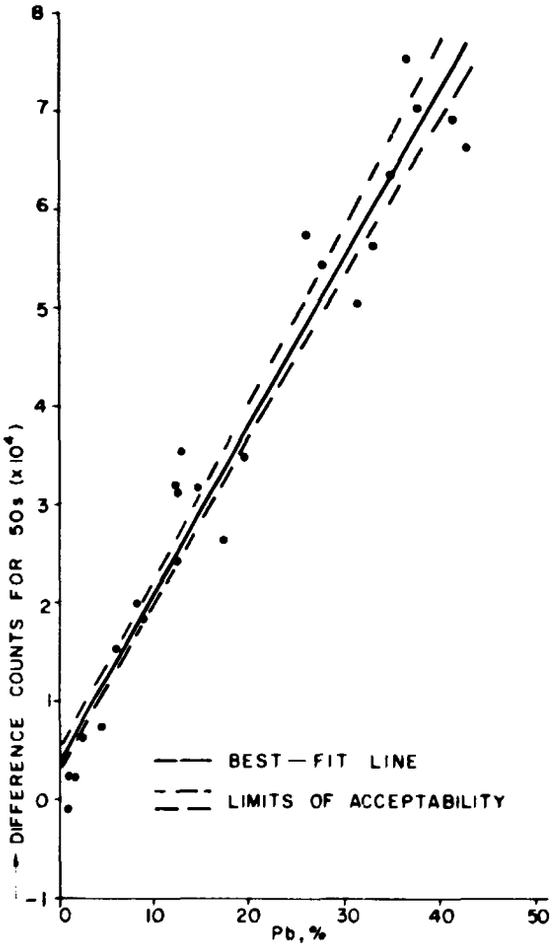

FIGURE 29 The determination of lead in 'intermediate' products

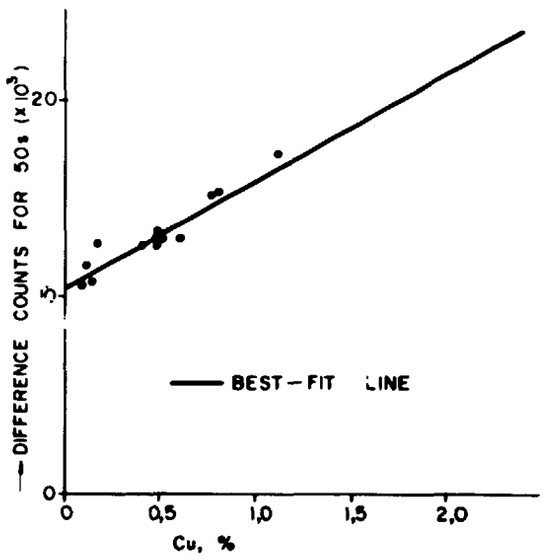

FIGURE 30 The determination of copper in low-grade materials

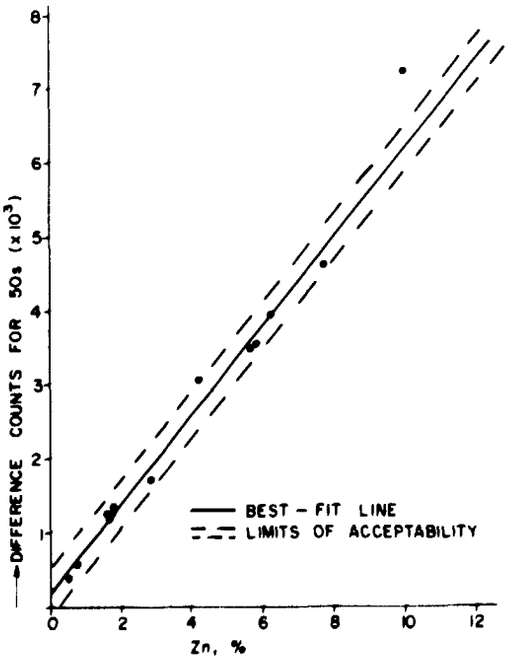

FIGURE 31 The determination of zinc in low-grade materials

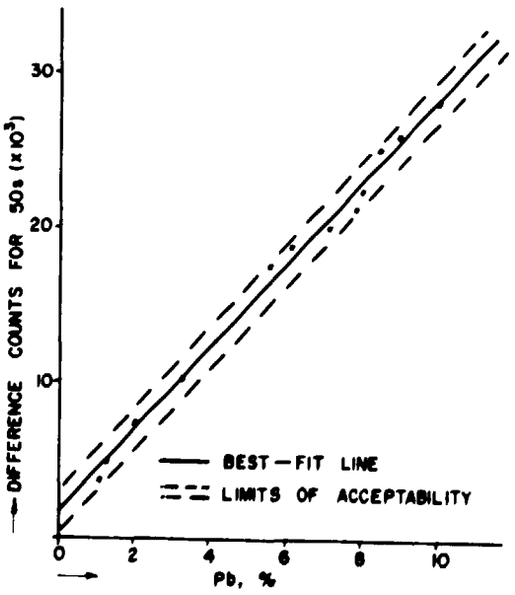

FIGURE 32 The determination of lead in low-grade materials

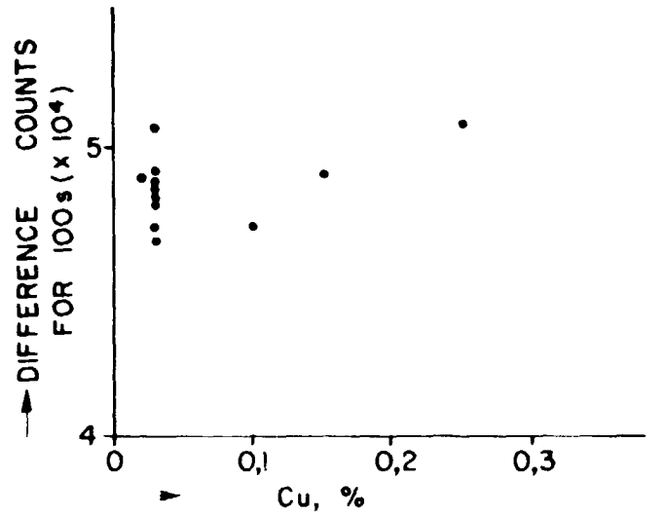

FIGURE 33 The determination of copper in tailing samples

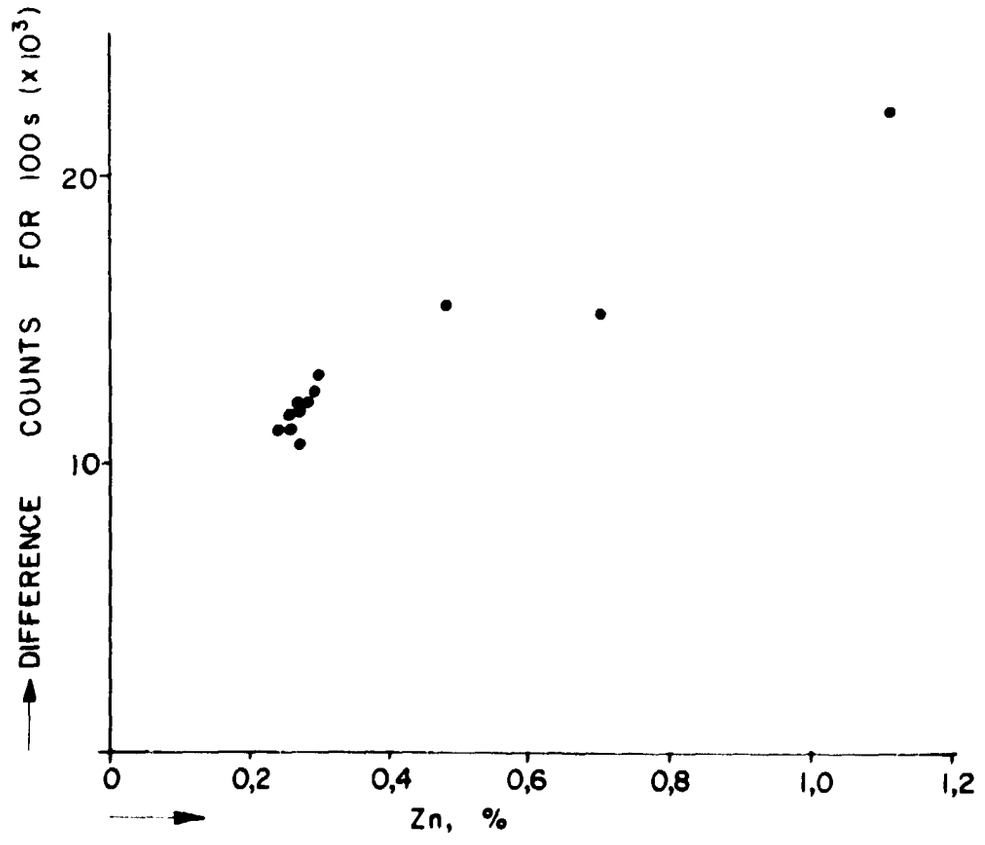

FIGURE 34 The determination of zinc in tailing samples

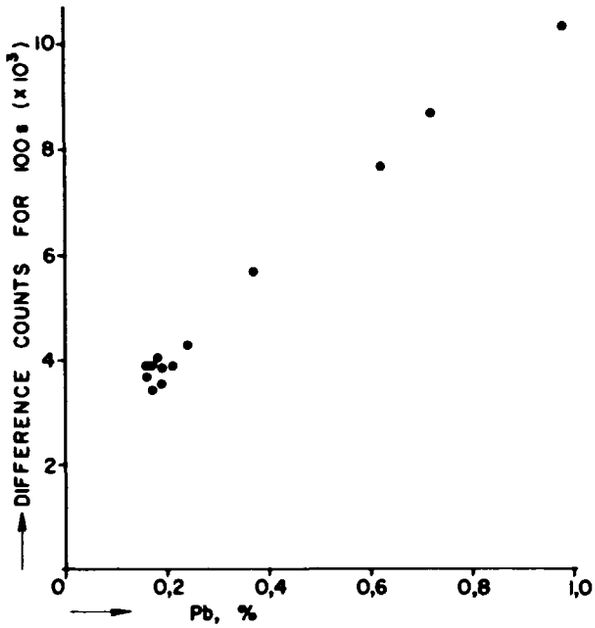

FIGURE 35 The determination of lead in tailing samples

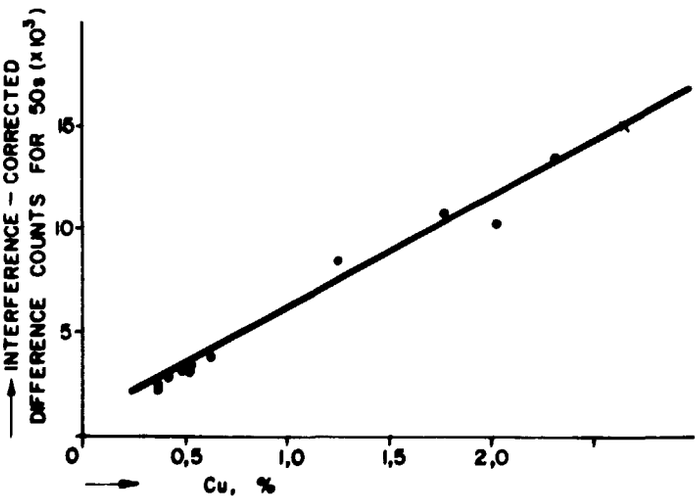

FIGURE 36 The determination, after correction for spectral interference, of copper in zinc concentrates

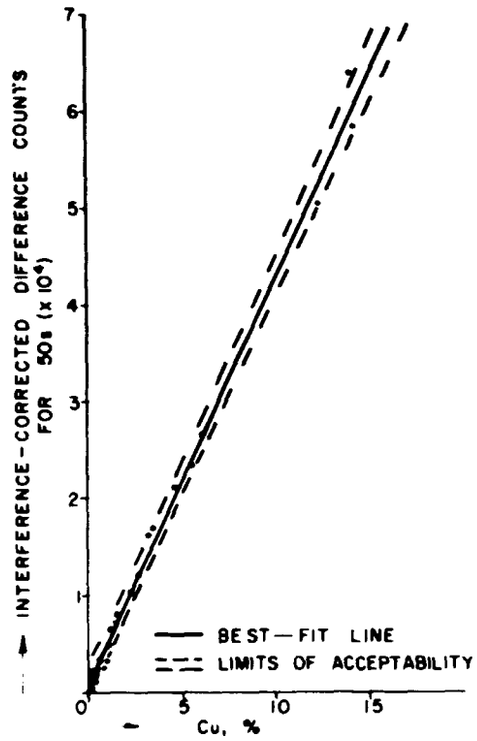

FIGURE 37 The determination, after correction for spectral interference, of copper in 'intermediate' products

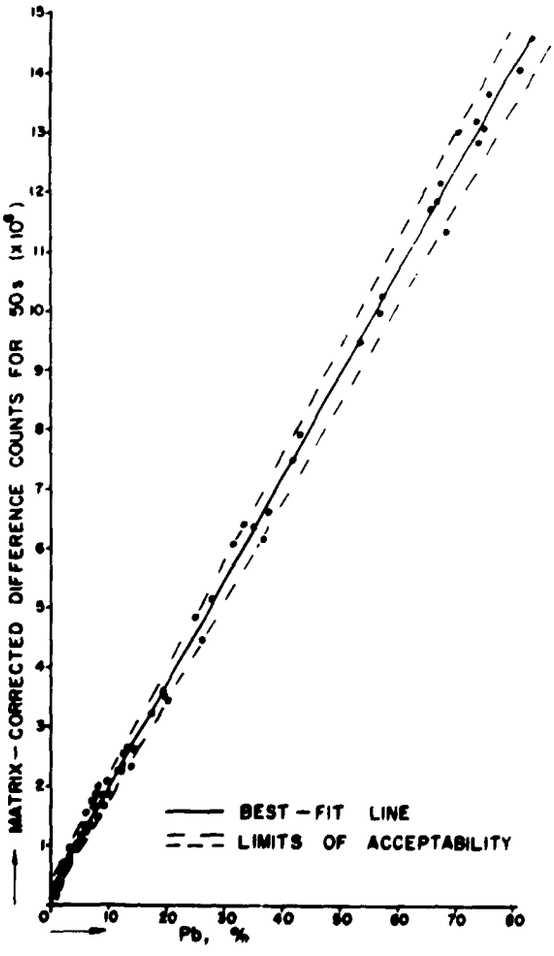

FIGURE 38 The determination, after correction for spectral interference and mass-absorption variations, of lead in sulphide ore products